Fine-Grained Scene Graph Generation with Data Transfer

Ao Zhang¹*, Yuan Yao²*, Qianyu Chen², Wei Ji¹, Zhiyuan Liu², Maosong Sun², Tat-Seng Chua¹ Department of Computer Science, National University of Singapore, Singapore

²Department of Computer Science and Technology

Institute for Artificial Intelligence, Tsinghua University, Beijing, China

Beijing National Research Center for Information Science and Technology, China

aozhang@u.nus.edu, yuan-yao18@mails.tsinghua.edu.cn

Abstract

Scene graph generation (SGG) aims to extract (subject, predicate, object) triplets in images. Recent works have made a steady progress on SGG, and provide useful tools for high-level vision and language understanding. However, due to the data distribution problems including longtail distribution and semantic ambiguity, the predictions of current SGG models tend to collapse to several frequent but uninformative predicates (e.g., on, at), which limits practical application of these models in downstream tasks. To deal with the problems above, we propose a novel Internal and External Data Transfer (IETrans) method, which can be applied in a play-and-plug fashion and expanded to large SGG with 1,807 predicate classes. Our IETrans tries to relieve the data distribution problem by automatically creating an enhanced dataset that provides more sufficient and coherent annotations for all predicates. By training on the transferred dataset, a Neural Motif model doubles the macro performance while maintaining competitive micro performance. The data and code for this paper are publicly available at https://github.com/ waxnkw/IETrans-SGG.pytorch.

1. Introduction

Scene graph generation (SGG) aims to detect relational triplets (e.g., (man, riding, bike)) in images. As an essential task for bridging the gap between vision and language, it can serve as a fundamental tool for high-level vision and language tasks, such as visual question answering [2, 24], image captioning [30, 7], and image retrieval [10, 26]. However, existing SGG methods can only make correct predictions on a limited number of predicate classes (e.g., 29 out of 50 pre-defined classes [34]), among which a lot of predicates are trivial and uninformative (e.g., on, and,

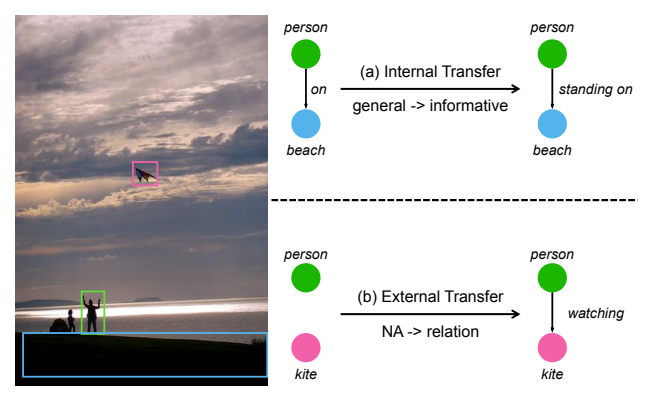


Figure 1. Generate an enhanced dataset automatically for better model training with: (a) **Internal Transfer**: Specify general predicate annotations as informative ones. (b) **External Transfer**: Relabel missed relations for NA.

near). This undermines the application of SGG for downstream tasks. To address the limitation, we first try to figure out two main problems we need to deal with:

- Long-tail problem: it refers to the phenomenon that annotations mainly concentrate on a few head predicate classes, and are much sparse on most tail predicate classes. For example, in Visual Genome, there are over 100K samples for the top 5 predicate classes, while over 90% of predicate classes have less than 10 samples. As a result, the performance of tail predicate classes is poor due to the lack of effective supervision.
- Semantic ambiguity: there exist some data samples that can be described as either general predicate class (e.g., on) or informative predicate class (e.g., riding). However, data annotators prefer some general predicate classes to informative ones for simplicity. This causes conflicts in single-label optimization since different labels are annotated for the same type of instances. In this condition, even when the informative predicates have enough training samples, the

^{*} indicates equal contribution

prediction will easily collapse to the general one.

To address the above mentioned problems, recent works propose to use resampling [6, 13], reweighting [29], and post-processing methods [22, 8] on predictions. We argue that these problems can be better alleviated by enhancing the existing dataset, which contains more abundant training samples for tail classes and also provides coherent annotations for different predicate classes.

Thus, we propose an Internal and External data Transfer (IETrans) method, which can be equipped to different baseline models. As shown in Figure 1, we automatically transfer data from general predicates to informative ones (Internal Transfer) and relabel relational triplets missed by annotators (External Transfer): (1) For internal trans**fer**, we first identify the general-informative relational pairs based on the confusion matrix, and then conduct a tripletlevel data transfer from general ones to informative ones. The internal transfer will not only alleviate the optimization conflict caused by semantic ambiguity but also provide more data for tail classes; (2) For external transfer, there exist many positive samples missed by annotators [12, 18], which are usually treated as negative samples by current methods. However, this kind of data can be considered as a potential data source, covering a wide range of predicate categories. Therefore, we also consider the NA samples, which are the set of negative and missed annotated samples. The missed annotated samples can be relabeled to provide more training samples.

It is worth noting that both internal transfer and external transfer are indispensable for improving SGG performance. Without the internal transfer, the external transfer will suffer from the semantic ambiguity problem. Meanwhile, the external transfer can further provide training samples for tail classes, especially for those that have a less semantic connection with head classes.

Through exhaustive experiments, we show that our method is both generalizable to different baseline models and scalable to large-scale SGG. We equip our data augmentation method with 4 different baseline models and find that it can significantly boost all models' macro performance with a very small discount on micro performance. For example, the macro performance of a Neural Motif model can be doubled with minor drop for micro performance on VG-50 [28] benchmark, which contains 50 predicate classes.

We additionally propose a new benchmark with 1,807 classes (VG-1800), which is more practical and challenging. To provide a reliable and stable evaluation, we manually remove unreasonable predicate classes and make sure there are over 5 samples for each predicate class on the test set. On VG-1800, our method shows significant superiority compared with baselines. The proposed IETrans can make correct predictions on 467 categories, compared

with all other baselines that can only correctly predict less than 70 categories. When the baseline model can only predict relations like (*cloud*, in, *sky*) and (*window*, on, *building*), our method can generate more informative ones like (*cloud*, floating through, *sky*) and (*window*, on exterior of, *building*).

Our main contributions are summarized as follows: (1) To cope with the long-tail problem and semantic ambiguity in SGG, we propose a novel IETrans method to generate an enhanced training set, which can be applied in a plug-and-play fashion. (2) We additionally propose a new data split VG-1800, which can provide reliable and stable evaluation for large-scale SGG. (3) Comprehensive experiments demonstrate the effectiveness of our IETrans in training SGG models, which can be shown by the SOTA performance on both VG-50 and VG-1800 benchmarks.

2. Related Work

2.1. Scene Graph Generation

As an important tool for bridging the gap between vision and language, SGG [17, 28, 18, 23, 34, 14] has drawn widespread attention from the community. SGG is first proposed as visual relation detection (VRD) [18], in which each relation is detected independently. Considering that relations are highly dependent on their context, [28] further proposes to formulate VRD as a dual-graph generation task, which can incorporate context information. Based on [28], different methods [17, 23, 34] are proposed to refine the object and relation representations in the scene graph. For example, [17] proposes a novel message passing mechanism that can encode edge directions into node representations.

2.2. Informative Scene Graph Generation

Although making steady progress on improving recall on SGG task, [23, 3] point out that the predictions of current SGG models are easy to collapse to several general and trivial predicate classes. Instead of only focusing on recall metric, [23, 3] propose a new metric named mean recall, which is the average recall of all predicate classes. [22] employs a causal inference framework, which can eliminate data bias during the inference process. CogTree [32] proposes to leverage the semantic relationship between different predicate classes, and design a novel CogTree loss to train models that can make informative predictions. In BGNN [13], the authors design a bi-level resampling strategy, which can help to provide a more balanced data distribution during the training process. However, previous works of designing new loss or conducting resampling, only focus on predicate-level adjustment, while the visual relation is triplet-level. For example, given the subject man and object skateboard, the predicate riding is an informative version of standing on, while given the subject man and object horse, riding will not be an informative alternative of standing on. Thus, instead of using less precise predicate-level manipulation, we employ a triplet-level transfer.

2.3. Large-scale Scene Graph Generation

In the last few years, there already exist some works [1, 36, 35, 31] focusing on large-scale SGG, for which how to provide a reliable evaluation is an important problem. [35] first proposes to study large-scale scene graph generation and makes a new split of Visual Genome dataset named VG80K, which contains 29,086 predicate categories. However, the annotations are too noisy to provide reliable evaluation. To cope with this problem, [1] further cleans the dataset, and finally reserves 2,000 predicate classes. However, only 1,429 predicate classes are contained in the test set, among which 903 relation categories have no more than 5 samples. To provide enough samples for each predicate class' evaluation, we re-split the Visual Genome to ensure each predicate class on the test set has more than 5 samples, and the total predicate class number is 1,807. For the proposed methods, [35] employs a triplet loss to regularize the visual representation with the constraint on word embedding space. RelMix [1] proposes to conduct data augmentation with the format of feature mixup. Visual distant supervision [31] pretrains the model on relabeled NA data with the help of a knowledge base and achieve improvement on a well-defined VG setting without semantic ambiguity. However, the data extension will be significantly limited by the semantic ambiguity problem. To deal with this problem, we also propose an internal transfer method to generate informative triplets.

3. Method

In this section, we first introduce the internal data transfer and external data transfer, respectively, and then elaborate how to utilize them collaboratively. Figure 2 shows the pipeline of our proposed IETrans.

The goal of our method is to generate an enhanced dataset automatically, which should provide more training samples for tail classes, and also specify general predicate classes as informative ones. Concretely, as shown in Figure 1, the general relation on between (*person*, *beach*) need to be specified as more informative one standing on, and the missed annotations between (*person*, *kite*) can be labeled so as to provide more training samples.

3.1. Problem Definition

Scene Graph Generation. Given an image I, a scene graph corresponding to I has a set of objects $O = \{(b_i, c_i)\}_{i=1}^{N_o}$ and a set of relational triplets $E = \{(s_i, p_i, o_i)\}_{i=1}^{N_c}$. For each object (b_i, c_i) , it consists of an object bounding box

 $b_i \in \mathbb{R}^4$ and an object class c_i which belongs to the predefined object class set \mathcal{C} . With $s_i \in O$ and $o_i \in O$, p_i is defined as relation between them and belongs to the predefined predicate class set \mathcal{P} .

Inference. SGG is defined as a joint detection of objects and relations. Generally, an SGG model will first detect the objects in the image I. Based on the detected objects, a typical SGG model will conduct a feature refinement for objects and relation representation, and then classify the objects and relations.

3.2. Internal Data Transfer

The key insight of internal transfer is to transfer samples from general predicate classes to their corresponding informative ones, like the example shown in Figure 1. We split the process into 3 sub-steps, including (1) Confusion Pair Discovery: discover confused predicate pairs as candidate general-informative pairs for given subject and object classes. (2) Transfer Pair Judgement: judge whether the candidate pair is valid. (3) Triplet Transfer: transfer data from the selected general predicate class to the corresponding informative one.

Confusion Pair Discovery. To find general predicate classes and corresponding informative ones, a straightforward way is to annotate the possible relation transitions manually. However, relations are highly dependent on the subject and object classes, i.e. relation is triplet-level rather than predicate-level. For example, (man, riding, bike) can be considered as an informative version of (man, sitting on, bike), while (man, riding, skateboard) can only be considered as an sub-type of (man, standing on, skateboard). In this condition, even under 50 predicate classes settings, the possible relation elements will scale up to an infeasible number for human annotation. Another promising alternative is to employ pre-defined knowledge bases, such as WordNet [19] and VerbNet [11]. However, existing knowledge bases are not specifically designed to cope with visual relation problems, which result in a gap between visual and textual hierarchies [25].

Thus, in this work, we try to specify the general-informative pairs by taking advantage of information within the dataset, and leave the use of external knowledge sources for future work. A basic assumption is that **informative predicate classes are easily confused by general ones**. Thus, we can first find confusion pairs as candidate general-informative pairs. Through observing the prediction results of the pre-trained Motif [34] model, we find that the collapse from informative predicate classes to general ones appears not only on the test set but also on the training set. As shown in Figure 3, the predicate classes riding and sitting on are significantly confused by a more general predicate class on.

On the training set, given a relational triplet class

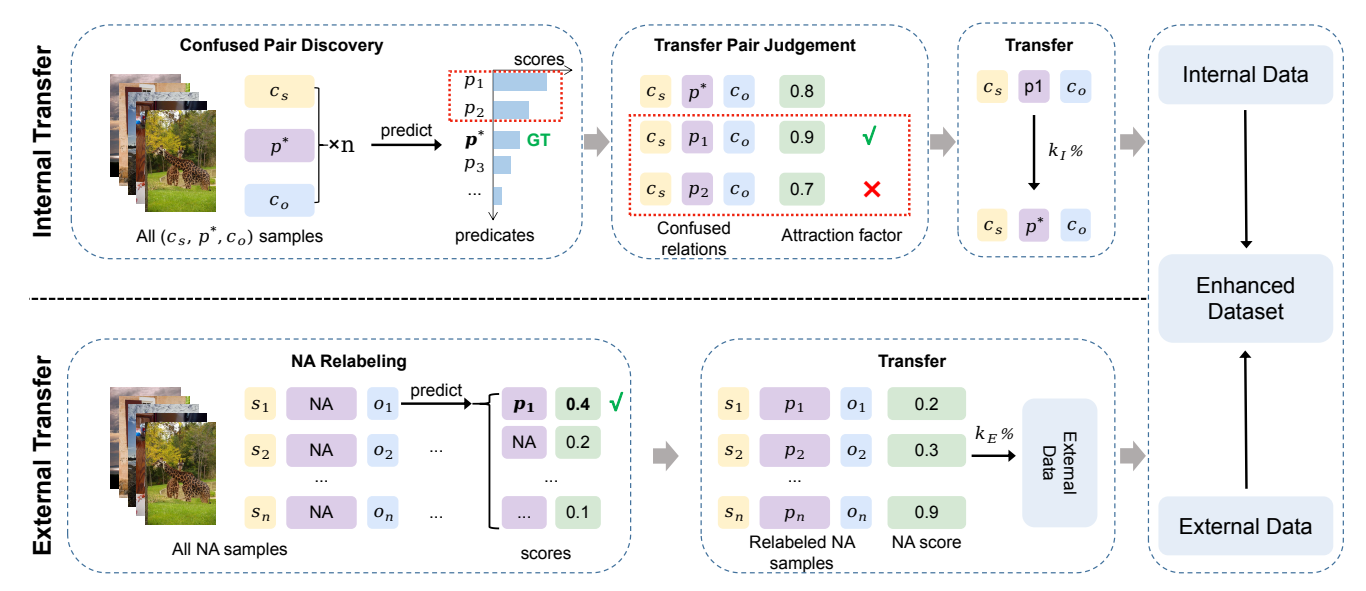


Figure 2. Illustration of our proposed IETrans to generate an enhanced dataset. **Internal transfer** is designed to transfer data from general predicate classes to informative ones. **External transfer** is designed to relabel NA data. To avoid misunderstanding, (c_s, p^*, c_o) is a relational triplet class representing samples with the subject class c_s , predicate class p^* , and object class c_o . (s_i, p_i, o_i) represent a single relational triplet instance.

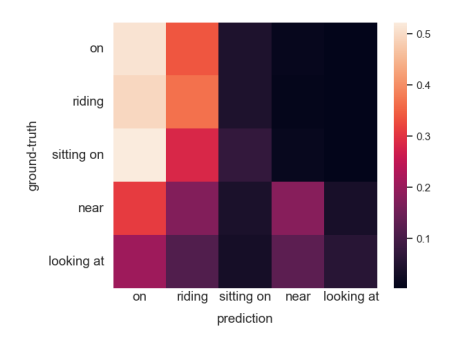


Figure 3. Confusion matrix of Motif [34]'s prediction score on all entity pairs in VG training set with the subject *man* and the object *motorcycle*.

 (c_s, p, c_o) , we use a pre-trained baseline model to predict predicate labels of all samples belonging to (c_s, p, c_o) , and average their score vectors. We denote the aggregated scores for all predicates as $S = \{s_{p_i} | p_i \in \mathcal{P}\}$. From S, we select all predicate classes with higher prediction scores than the ground-truth annotation p, which can be formulated as $\mathcal{P}_c = \{p_i | s_{p_i} > s_p\}$. \mathcal{P}_c can be considered as the most confusing predicate set for p, which can serve as candidate transfer sources.

Transfer Pair Judgement. However, a confused predicate class does not equal to a general one. Sometimes, a general predicate can also be confused by an informative predicate. For example, in Figure 3, under the constraint of $c_s = man$ and $c_o = motorcycle$, the less informative predicate sitting on is confused by the more informative predicate riding. In this condition, it not a good choice

to transfer from riding to sitting on. Thus, we need to further select the truly general predicates from the candidate set \mathcal{P}_c .

To select the most possible general predicate classes from \mathcal{P}_c , we first introduce an important feature that is useful to recognize general predicate classes. As observed by [32], the general predicate classes usually cover more diverse relational triplets, while informative ones are limited. Based on this observation, we can define the attraction factor of a triplet category (c_s, p, c_o) as:

$$A(c_s, p, c_o) = \frac{1}{\sum_{c_i, c_j \in \mathcal{C}} \mathcal{I}(c_i, p, c_j)},$$
 (1)

where C is the object categories set and $\mathcal{I}(t)$ indicates whether the triplet category t exists in the training set, which can be formulated as:

$$\mathcal{I}(t) = \begin{cases} 1, & \text{if } t \in \text{training set} \\ 0, & \text{otherwise} \end{cases}$$
(2)

The denominator of $A(c_s,p_i,c_o)$ is the number of relational triplets containing p_i . Thus, $A(c_s,p_i,c_o)$ with smaller value means p_i is more likely to be a general predicate. Concretely, when $A(c_s,p_i,c_o) < A(c_s,p,c_o)$, we transfer data from (c_s,p_i,c_o) to (c_s,p,c_o) .

However, only considering the number of relational triplet classes also has drawbacks: some relational triplets with very limited number of samples (*e.g.*, only 1 or 2 samples) might be annotation noise, while these relational triplets are easily selected as transfer targets. Transferring

too much data to such uncertain relational triplets will significantly degenerate models' performance. Thus, we further consider the number of each relational triplet and modify the attraction factor as:

$$A(c_s, p, c_o) = \frac{N(c_s, p, c_o)}{\sum_{c_i, c_j \in \mathcal{C}} \mathcal{I}(c_i, p, c_j) \cdot N(c_i, p, c_j)}, \quad (3)$$

where N(t) denote the number of instances with relational type t in the training set. With the attraction factor, we can further filter the candidate confusion set \mathcal{P}_c to the valid transfer source for (c_s, p, c_o) :

$$\mathcal{P}_s = \{ p_i | (p_i \in \mathcal{P}_c) \land (A(c_s, p_i, c_o) < A(c_s, p, c_o)) \},$$
(4)

where \wedge denotes the logical conjunction operator.

Triplet Transfer. Given the transfer source \mathcal{P}_s , we collect all samples in the training set satisfying:

$$T = \{(o_i, p_k, o_j) | (c_{o_i} = c_s) \land (p_k \in \mathcal{P}_s) \land (c_{o_j} = c_o) \}.$$
(5)

Then, we sort T by model's prediction score of p, and transfer the top $k_I\%$ samples to the target triplet category (c_s, p, c_o) . Note that, a triplet instance may need to be transferred to over 1 relational triplets. To deal with the conflict, we choose the target predicate with the highest attraction factor.

3.3. External Data Transfer

The goal of our external transfer is to relabel unannotated samples to excavate missed relational triplets, like the example shown in Figure 1.

NA Relabeling. NA samples refers to all unannotated samples in the training set, including both truly negative samples and missed positive samples. In external transfer, NA samples are directly considered as the transfer source and are relabeled as existing relational triplet types.

To get the NA samples, we first traverse all unannotated object pairs in images. However, considering data transfer from all NA samples to all possible predicate classes will bring heavy computational burden, and inevitably increase the difficulty of conducting precise transfer, which will lower the transferred data quality. Thus, we only focus on object pairs whose bounding boxes have overlaps and limit the possible transfer targets to existing relational triplet types. The exploration of borrowing zero-shot relational triplets from NA is left for future work.

Given a sample (s, NA, o), we can get its candidate target predicate set as:

$$Tar(s, NA, o) = \{ p | (p \in \mathcal{P}) \land (N(c_s, p, c_o) > 0) \land (IoU(b_s, b_o) > 0) \}$$

$$(6)$$

where \mathcal{P} denotes pre-defined predicate classes, b_s and b_o denote bounding boxes of s and o, and IoU denotes the intersection over union.

Given a triplet (s, NA, o), the predicate class with the highest prediction score except for NA is chosen. The label assignment can be formulated as:

$$p = \underset{p \in Tar(s, NA, o)}{\operatorname{arg}} (\phi^{p}(s, o)), \tag{7}$$

where $\phi^p(\cdot)$ denotes the prediction score of predicate p.

NA Triplet Transfer. To decide transfer or not, we rank all chosen (s, NA, o) samples according to NA scores in an ascending order. The lower NA score means the sample is more likely to be a missed positive sample. Similar with internal transfer, we simply transfer the top $k_E\%$ data.

3.4. Combination

Internal transfer is conducted on annotated data and external transfer is conducted on unannotated data, which are orthogonal to each other. Thus, we can simply merge the data without conflicts. After obtaining the enhanced dataset, we re-train a new model from scratch and use the new model to make inferences on the test set.

4. Experiments

In this section, we first show the generalizability of our method with different baseline models and the expansibility to large-scale SGG. We also do ablation studies to explore the influence of different modules and hyperparameters. Finally, analysis is conducted to show the effectiveness of our method in enhancing the current dataset.

4.1. Generalizability with Different Models

We first validate the generalizability of our method with different baseline models and its effectiveness when compared with current SOTA methods.

Datasets. Popular VG-50 [28] benchmark is employed, which consists of 50 predicate classes and 150 object classes.

Tasks. Following previous works [28, 22, 34], we evaluate our model on three widely used SGG tasks: (1) Predicate Classification (PREDCLS) provides both localization and object classes, and requires models to recognize predicate classes. (2) Scene Graph Classification (SGCLS) provides only correct localization and asks models to recognize both object and predicate classes. (3) In Scene Graph Detection (SGDET), models are required to first detect the bounding boxes and then recognize both object and predicate classes.

Metrics. Following previous works [32, 23], we use Recall@K (**R**@**K**) and mean Recall@K (**m**R@**K**) as our metrics. However, different trade-offs between R@K and mR@K are made in different methods, which makes it hard to make a direct comparison. Therefore, we further

	Models	Predicate Classification			Scene Graph Classification			Scene Graph Detection		
		R@50 / 100	mR@50 / 100	F@50 / 100	R@50 / 100	mR@50	F@50 / 100	R@50 / 100	mR@50 / 100	F@50 / 100
Specific	KERN [4]	65.8 / 67.6	17.7 / 19.2	27.9 / 29.9	36.7 / 37.4	9.4 / 10.0	15.0 / 15.8	27.1 / 29.8	6.4 / 7.3	10.4 / 11.7
	GBNet [33]	66.6 / 68.2	22.1 / 24.0	33.2 / 35.5	37.3 / 38.0	12.7 / 13.4	18.9 / 19.8	26.3 / 29.9	7.1 / 8.5	11.2 / 13.2
	BGNN [13]	59.2 / 61.3	30.4 / 32.9	40.2 / 42.8	37.4 / 38.5	14.3 / 16.5	20.7 / 23.1	31.0 / 35.8	10.7 / 12.6	15.9 / 18.6
	DT2-ACBS [6]	23.3 / 25.6	35.9 / 39.7	28.3 / 31.1	16.2 / 17.6	24.8 / 27.5	19.6 / 21.5	15.0 / 16.3	22.0 / 24.0	17.8 / 19.4
	PCPL [29]	50.8 / 52.6	35.2 / 37.8	41.6 / 44.0	27.6 / 28.4	18.6 / 19.6	22.2 / 23.2	14.6 / 18.6	9.5 / 11.7	11.5 / 14.4
	Motif [34]	64.0 / 66.0	15.2 / 16.2	24.6 / 26.0	38.0 / 38.9	8.7 / 9.3	14.2 / 15.0	31.0 / 35.1	6.7 / 7.7	11.0 / 12.6
	-TDE [22]	46.2 / 51.4	25.5 / 29.1	32.9 / 37.2	27.7 / 29.9	13.1 / 14.9	17.8 / 19.9	16.9 / 20.3	8.2 / 9.8	11.0 / 13.2
	-CogTree [32]	35.6 / 36.8	26.4 / 29.0	30.3 / 32.4	21.6 / 22.2	14.9 / 16.1	17.6 / 18.7	20.0 / 22.1	10.4 / 11.8	13.7 / 15.4
	-EBM [21]	-/-	18.0 / 19.5	-/-	-/-	10.2 / 11.0	-/-	-/-	7.7 / 9.3	-/-
	-DeC [9]	-/-	35.7 / 38.9	-/-	-/-	18.4 / 19.1	-/-	-/-	13.2 / 15.6	-/-
	-DLFE [5]	52.5 / 54.2	26.9 / 28.8	35.6 / 37.6	32.3 / 33.1	15.2 / 15.9	20.7 / 21.5	25.4 / 29.4	11.7 / 13.8	16.0 / 18.8
	-IETrans (ours)	54.7 / 56.7	30.9 / 33.6	39.5 / 42.2	32.5 / 33.4	16.8 / 17.9	22.2 / 23.3	26.4 / 30.6	12.4 / 14.9	16.9 / 20.0
	-IETrans+Rwt (ours)	48.6 / 50.5	35.8 / 39.1	41.2 / 44.1	29.4 / 30.2	21.5 / 22.8	24.8 / 26.0	23.5 / 27.2	15.5 / 18.0	18.7 / 21.7
.2	VCTree [23]	66.2 / 68.1	14.9 / 16.1	24.3 / 26.0	40.5 / 41.4	7.5 / 7.9	12.7 / 13.3	31.5 / 36.2	5.7 / 6.9	9.7 / 11.6
Model-Agnostic	-TDE [22]	47.2 / 51.6	25.4 / 28.7	33.0 / 36.9	25.4 / 27.9	12.2 / 14.0	16.5 / 18.6	19.4 / 23.2	9.3 / 11.1	12.6 / 15.0
	-CogTree [32]	44.0 / 45.4	27.6 / 29.7	33.9 / 35.9	30.9 / 31.7	18.8 / 19.9	23.4 / 24.5	18.2 / 20.4	10.4 / 12.1	13.2 / 15.2
	-EBM [21]	-/-	18.2 / 19.7	-/-	-/-	12.5 / 13.5	-/-	-/-	7.7 / 9.1	-/-
	-DLFE [5]	51.8 / 53.5	25.3 / 27.1	34.0 / 36.0	33.5 / 34.6	18.9 / 20.0	24.2 / 25.3	22.7 / 26.3	11.8 / 13.8	15.5 / 18.1
	-IETrans (ours)	53.0 / 55.0	30.3 / 33.9	38.6 / 41.9	32.9 / 33.8	16.5 / 18.1	22.0 / 23.6	25.4 / 29.3	11.5 / 14.0	15.8 / 18.9
	-IETrans+Rwt (ours)	48.0 / 49.9	37.0 / 39.7	41.8 / 44.2	30.0 / 30.9	19.9 / 21.8	23.9 / 25.6	23.6 / 27.8	12.0 / 14.9	15.9 / 19.4
	GPS-Net [17]	64.4 / 66.7	19.2 / 21.4	29.6 / 32.4	37.5 / 38.6	11.7 / 12.5	17.8 / 18.9	27.8 / 32.1	7.4 / 9.5	11.7 / 14.7
	-DeC [9]	-/-	35.9 / 38.4	-/-	-/-	17.4 / 18.5	-/-	-/-	11.2 / 15.2	-/-
	-IETrans (ours)	52.3 / 54.3	31.0 / 34.5	38.9 / 42.2	31.8 / 32.7	17.0 / 18.3	22.2 / 23.5	25.9 / 28.1	14.6 / 16.5	18.7 / 20.8
	-IETrans+Rwt (ours)	47.5 / 49.4	34.9 / 38.6	40.2 / 43.3	29.3 / 30.3	19.8 / 21.6	23.6 / 25.2	23.1 / 25.0	16.2 / 18.8	19.0 / 21.5
	Transformer [22]	65.6 / 67.3	16.3 / 17.6	26.1 / 27.9	40.2 / 41.0	10.1 / 10.7	16.1 / 17.0	33.0 / 37.4	8.1 / 9.6	13.0 / 15.3
	-CogTree [32]	38.4 / 39.7	28.4 / 31.0	32.7 / 34.8	22.9 / 23.4	15.7 / 16.7	18.6 / 19.5	19.5 / 21.7	11.1 / 12.7	14.1 / 16.0
	-IETrans (ours)	51.8 / 53.8	30.8 / 34.7	38.6 / 42.2	32.6 / 33.5	17.4 / 19.1	22.7 / 24.3	25.5 / 29.6	12.5 / 15.0	16.8 / 19.9
	-IETrans+Rwt (ours)	49.0 / 50.8	35.0 / 38.0	40.8 / 43.5	29.6 / 30.5	20.8 / 22.3	24.4 / 25.8	23.1 / 27.1	15.0 / 18.1	18.2 / 21.7

Table 1. Performance (%) of our method and other baselines on VG-50 dataset. **IETrans** denotes different models equipped with our IETrans. **Rwt** denotes using the reweighting strategy.

Models	Top-1			Top-5			Top-10					
1.1040.15	Acc	mAcc	F-Acc	Non-Zero	Acc	mAcc	F-Acc	Non-Zero	Acc	mAcc	F-Acc	Non-Zero
BGNN [13]	58.73	0.61	1.21	42	83.83	2.44	4.74	96	88.48	3.75	7.20	127
Motif [34]	59.63	0.61	1.21	47	84.82	2.68	5.20	112	89.44	4.37	8.33	139
-Focal Loss	54.65	0.26	0.52	14	79.69	0.79	1.56	27	85.21	1.36	2.68	41
-TDE [22]	60.00	0.62	1.23	45	85.29	2.77	5.37	119	89.92	4.65	8.84	152
-RelMix [13]	60.16	0.81	1.60	65	85.31	3.27	6.30	134	89.91	5.17	9.78	177
-IETrans ($k_I=10\%$) (ours)	56.66	1.89	3.66	202	83.99	8.23	14.99	419	89.71	13.06	22.80	530
-IETrans $(k_I=90\%)$ (ours)	27.40	4.70	8.02	467	72.48	13.34	22.53	741	83.50	19.12	31.12	865

Table 2. Performance of our method and baselines on VG-1800 dataset. **IETrans** denotes the Motif [34] model trained using our IETrans. To better compare with baselines, we show different Acc and mAcc trade-offs by setting different k_I .

propose an overall metric F@K to jointly evaluate R@K and mR@K, which is the harmonic average of R@K and mR@K.

Baselines. We categorize several baseline methods into two categories: (1) **Model-agnostic baselines.** They refers to methods that can be applied in a plug-and-play fashion. For this part, we include TDE [22], CogTree [32], EBM [21], DeC [9], and DLFE [5]. (2) **Specific models.** We also include some dedicated designed models with strong performance, including KERN [4], GBNet [33], BGNN [13], DT2-ACBS [6], and PCPL [29].

Implementation Details. Following [22], we employ a pretrained Faster-RCNN [20] with ResNeXt-101-FPN [15, 27]

backbone. In the training process, the parameters of the detector are fixed to reduce the computation cost. The batch size is set to 12, and the learning rate is 0.12. We optimize all models with an SGD optimizer. We decrease the learning rate 3 times by the factor of 10 until the end of training. Specifically, to better balance the data distribution, the external transfer will not be conducted for the top 15 frequent predicate classes. To avoid deviating too much from the original data distribution, all frequency bias items are calculated from the original dataset. For internal and external transfer, the k_I is set to 70% and k_E is set to 100%.

Comparison with SOTAs. We report the results of our IETrans and baselines for VG-50 in Table 1. Based on the

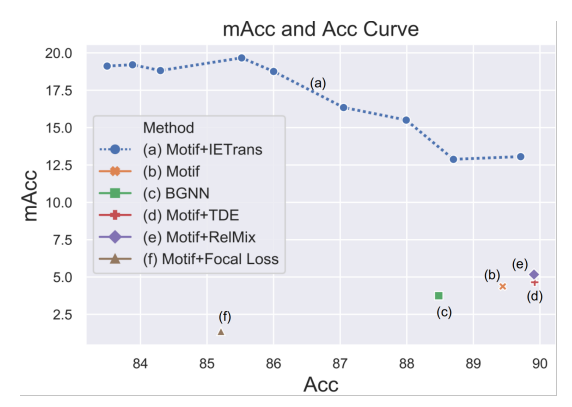


Figure 4. The mAcc and Acc curve. (a) is our IETrans method. k_I is tuned to generate the blue curve. (b-f) are baselines.

observation of experimental results, we have summarized the following conclusions:

Our IETrans is capable of generalizing to different baseline models. We equip our method with 4 different models, including Motif [34], VCTree [23], GPS-Net [17], and Transformer [22]. The module architectures range from conventional CNN to TreeLSTM (VCTree) and self-attention layers (Transformer). The training algorithm contains both supervised training and reinforcement learning (VCTree). Despite the model diversity, our IETrans can boost all models' mR@K metric while keeping competitive R@K performance. For example, our IETrans can double mR@50 and mR@100 across all 3 tasks for VCTree, while keeping a less than 20% discount on R@50 and R@100.

Compared with other model-agnostic methods, our IETrans outperforms all of them in nearly all metrics. For example, when applying IETrans to Motif on PRED-CLS, our model can achieve the highest R@50/100 and mR@50/100 among all model-agnostic baselines except for DeC. After adding the reweighting strategy, our IETrans can outperform DeC on mR.

Compared with strong specific baselines, our method can also achieve competitive performance on R@50/100, mR@50/100, and best overall performance on F@50/100. Considering mR@50/100, our method with reweighting strategy is slightly lower than DT2-ACBS in SGCLS and SGDET task, while our method performs much better than them on R@50/100(e.g. 24.3 points of VCTree in PREDCLS task). For overall comparison considering F@50/100 metrics, our VCTree+IETrans+Rwt can achieve the best F@50/100 on PREDCLS and Motif+IETrans+Rwt achieves the best F@50/100 in SGCLS and SGDET task.

4.2. Expansibility to Large-Scale SGG

We also validate our IETrans on VG-1800 dataset to show its expansibility to large-scale scenarios.

Datasets. We re-split the Visual Genome dataset to create a VG-1800 benchmark, which contains 70,098 object

categories and 1,807 predicate categories. Different from previous large-scale VG split [35, 1], we clean the misspellings and unreasonable relations manually and make sure all 1,807 predicate categories appear on both training and test set. For each predicate category, there are over 5 samples on the test set to provide a reliable evaluation. Detailed statistics of VG-1800 dataset are provided in Appendix.

Tasks. Due to huge amount of object classes, including object detection will make it too hard to make correct triplet-level predictions, which obscures the evaluation of predicate recognition ability. In this work, we mainly focus on **PREDCLS** and leave the challenging object detection for future work.

Metrics. Following [35, 1], we use accuracy (**Acc**) and mean accuracy upon all predicate classes (**mAcc**). Similar to VG-50, the harmonic average of two metrics is reported as **F-Acc**. In addition, we also report the number of predicate classes that the model can make at least one correct prediction, and denote it as **Non-Zero**.

Baselines. We also include model-agnostic baselines including Focal Loss [16], TDE [22], and RelMix [1], and a specific model BGNN [13].

Implementation Details. Compared with VG-50, similar learning rate, backbones, learning schedules are used on VG-1800 dataset. Specially, due to the significant increase of (subject, predicate, object) combinations, we equally remove all frequency bias items on VG-1800 to reduce machines' memory usage. For internal and external transfer, the k_I is set to 90% and k_E is set to 100%.

Comparison with SOTAs. Performance of our method and baselines are shown in Table 2. Based on the observation of experimental results, we have summarized the following conclusions:

Our model can successfully work on large-scale settings. On VG-1800 dataset, the long-tail problem is even exacerbated, where hundreds of predicate classes have only less than 10 samples. In this condition, simply conducting resampling (BGNN) or increasing loss weight (Focal Loss) on tail classes can not work well. Different from these methods, our IETrans can successfully boost the performance on mAcc while keeping competitive results on Acc. For quantitative comparison, our IETrans ($k_I = 10\%$) can significantly improve the performance in top-10 mAcc (e.g., 19.12% vs. 4.37%) while maintaining comparable performance on Acc.

Compared with different baselines, our method can outperform them for overall evaluation. As shown in Table 2, our IETrans ($k_I = 90\%$) can achieve best performance on F-Acc, which is over 3 times of the second highest baseline, RelMix, a method specifically designed for large-scale SGG. Different from VG-50, we do not in-

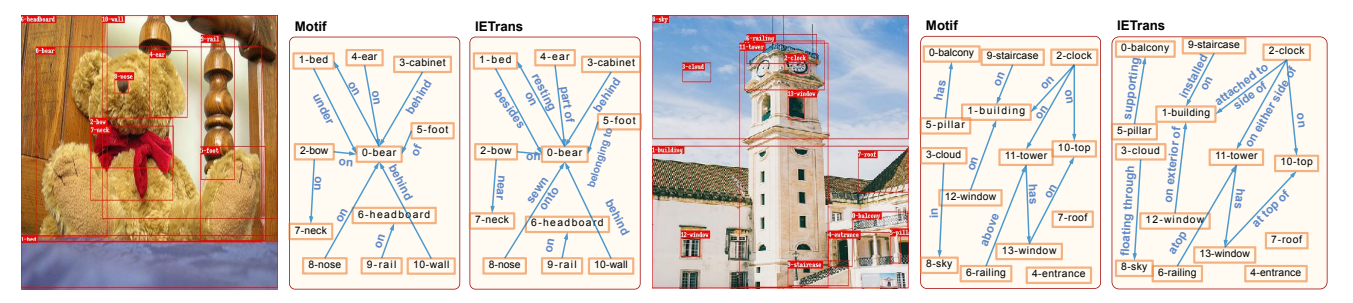


Figure 5. Visualization of raw Motif model and Motif equipped with our IETrans.

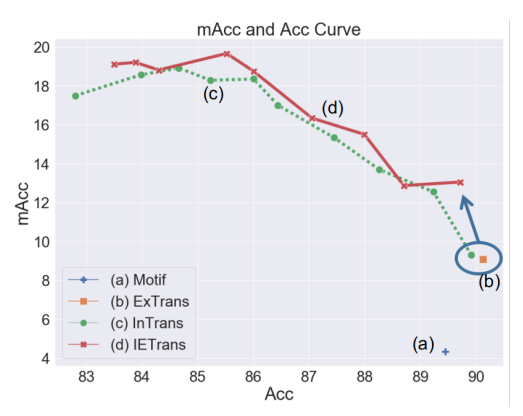


Figure 6. The mAcc and Acc curve. (a) Normally trained Motif. (b) ExTrans: external transfer. (c) InTrans: internal transfer. (d) IETrans is our proposed method. k_I is tuned to generate a curve. The blue circle and arrow mean that combining ExTrans and InTrans can lead to the pointed result.



Figure 7. (a) The influence of k_I in the Top-10 F-Acc when only conducting the internal transfer. (b) The influence of k_E in the Top-10 F-Acc when only conducting the external transfer.

clude IETrans+Rwt, because reweighting will decrease the model's overall performance, which might be caused by the severe noise problem in VG-1800's tail classes. To make the visualized comparison, we plot a curve of IETrans with different Acc and mAcc trade-offs by tuning k_I , and show the performance of other baselines as points. As shown in Figure 4, all baselines drawn as points are under our curve, which means our method can achieve better performance than them. Moreover, our IETrans ($k_I = 90\%$) can make correct predictions on 467 predicate classes for top-1 results, while the **Non-Zero** value of all other baselines are less than 70.

Case Studies. To show the potential of our method for real-world application, we provide some cases in Figure 5. We can observe that our IETrans can help to generate more informative predicate classes while keeping faithful to the image content. For example, when the Motif model only predict relational triplets like (foot, of, bear), (nose, on, bear) and (cloud, in, sky), our IETrans can generate more informative ones as (foot, belonging to, bear), (nose, sewn onto, bear), and (cloud, floating through, sky).

4.3. Ablation Studies

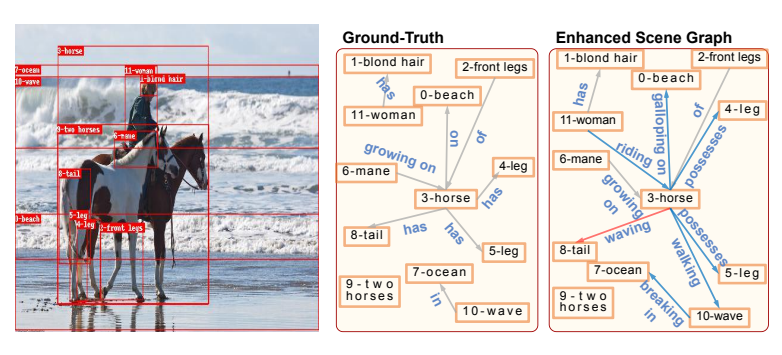
In this part, we investigate the influence of internal transfer, external transfer, and corresponding parameters, k_I and k_E .

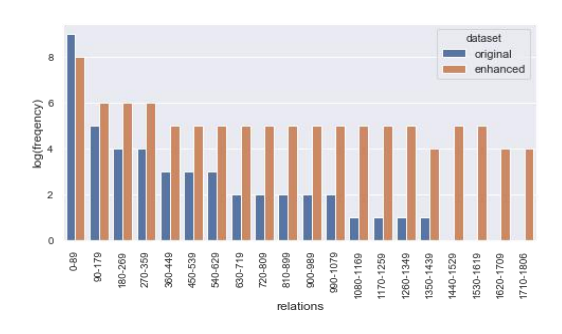
Influence of Internal Transfer. As shown in Figure 6, only using external transfer (yellow cube) is hard to boost the mAcc performance as much as IETrans. The reason is that although introducing samples for tail classes, they will still be suppressed by corresponding general ones. However, by introducing internal transfer (green point) to cope with semantic ambiguity problem, the performance (red cross) can be improved significantly on mAcc, together with minor performance drop on Acc.

Influence of External Transfer. Although internal transfer can achieve huge improvement on mAcc compared with Motif, its performance is poor compared with IETrans, which shows the importance of further introducing training data by external transfer. Combining two methods can maximize the advantages of data transfer.

Influence of k_I. As shown in Figure 7 (a), with the increase of k_I , the top-10 F-Acc will increase until $k_I = 80\%$, and begin to decrease when $k_I > 80\%$. The phenomenon indicates that a large number of general predicates can be interpreted as informative ones. Moving these predicates to informative ones will boost the overall performance. However, there also exists some predicates that can not be interpreted as informative ones or be modified suitably by current methods, which is harmful to the performance of models.

Influence of k_E. As shown in Figure 7 (b), the overall per-





(a) Enhanced Scene Graph Visualization

(b) Distribution Change

Figure 8. (a) **Enhanced Scene Graph Visualization.** Gray line denotes unchanged relation. Blue line denotes changed and reasonable relation. Red line denotes changed but unreasonable relation. (b) **Distribution Change.** The comparison between distributions of original dataset and enhanced dataset for VG-1800. The x-axis is the relation id intervals from head to tail classes. The y-axis is the corresponding log-frequency.

formance increases slowly with the initial 90% transferred data, but improves significantly with the rest 10%. Note that, the data is ranked according to the NA score, which means that the last 10% data is actually what the model considered as most likely to be truly negative. The phenomenon indicates that the model may easily classify tail classes as negative samples, while this part of data is of vital significance for improving the model's ability of making informative predictions.

4.4. Analysis of Enhanced Dataset

We further analyze the effectiveness of our proposed IETrans from the aspect of recognized visual hierarchy, correctness of the enhanced dataset, and the distribution change.

Visual Hierarchy Evaluation. A key element of conducting correct internal transfer is to find reasonable general-informative relation pairs. To evaluate the precision, we randomly choose 50 pairs with over 3 samples being transferred, so as to avoid involving too many noise-to-noise pairs. Then, human evaluation is conducted. The ratio of reasonable general-informative pairs is **76**% for VG-50, and **74**% for VG-1800. Please refer to the Appendix for concrete examples.

Enhanced Scene Graph Correctness. We also investigate the correctness of enhanced scene graphs from the instance level. Qualitatively, we give an example in Figure 8(a). Quantitatively, we randomly choose 100 changed relations, including both internal transferred and external transferred data, and make human evaluation on the correctness. The ratio of reasonable transferred data is 82% for VG-50, and 72% for VG-1800. We can see that the IETrans is less accurate on VG-1800, which indicates that it is more challenging to conduct precise data transfer on VG-1800.

Distribution Change. The distribution change is shown in

Figure 8(b). We can see that our IETrans can effectively supply samples for non-head classes.

5. Conclusion

In this paper, we design a data transfer method named IETrans to generate an enhanced dataset for the SGG. The proposed IETrans consists of an internal transfer module to relabel general predicate classes as informative ones and an external transfer module to complete missed annotations. Comprehensive experiments are conducted to show the effectiveness of our method. In the future, we hope to design more precise and adaptive data transfer schemas to reduce noise and also incorporate commonsense knowledge into the prediction process.

References

- [1] Sherif Abdelkarim, Aniket Agarwal, Panos Achlioptas, Jun Chen, Jiaji Huang, Boyang Li, Kenneth Church, and Mohamed Elhoseiny. Long tail visual relationship recognition with hubless regularized relmix. *arXiv preprint arXiv:2004.00436*, 2020. 3, 7, 12
- [2] Stanislaw Antol, Aishwarya Agrawal, Jiasen Lu, Margaret Mitchell, Dhruv Batra, C Lawrence Zitnick, and Devi Parikh. Vqa: Visual question answering. In *Proceedings of ICCV*, pages 2425–2433, 2015.
- [3] Tianshui Chen, Weihao Yu, Riquan Chen, and Liang Lin. Knowledge-embedded routing network for scene graph generation. In *Proceedings of CVPR*, pages 6163–6171, 2019.
- [4] Tianshui Chen, Weihao Yu, Riquan Chen, and Liang Lin. Knowledge-embedded routing network for scene graph generation. In *Proceedings of the IEEE/CVF Conference on Computer Vision and Pattern Recognition*, pages 6163–6171, 2019. 6
- [5] Meng-Jiun Chiou, Henghui Ding, Hanshu Yan, Changhu Wang, Roger Zimmermann, and Jiashi Feng. Recovering the

- unbiased scene graphs from the biased ones. In *Proceedings* of ACM Multimedia, pages 1581–1590, 2021. 6
- [6] Alakh Desai, Tz-Ying Wu, Subarna Tripathi, and Nuno Vasconcelos. Learning of visual relations: The devil is in the tails. In *Proceedings of ICCV*, pages 15404–15413, 2021. 2,
- [7] Jiuxiang Gu, Shafiq Joty, Jianfei Cai, Handong Zhao, Xu Yang, and Gang Wang. Unpaired image captioning via scene graph alignments. In *Proceedings of ICCV*, pages 10323– 10332, 2019. 1
- [8] Yuyu Guo, Lianli Gao, Xuanhan Wang, Yuxuan Hu, Xing Xu, Xu Lu, Heng Tao Shen, and Jingkuan Song. From general to specific: Informative scene graph generation via balance adjustment. In *Proceedings of ICCV*, pages 16383– 16392, 2021. 2
- [9] Tao He, Lianli Gao, Jingkuan Song, Jianfei Cai, and Yuan-Fang Li. Semantic compositional learning for low-shot scene graph generation. *Proceedings of ICCV*, 2021. 6
- [10] Justin Johnson, Ranjay Krishna, Michael Stark, Li-Jia Li, David Shamma, Michael Bernstein, and Li Fei-Fei. Image retrieval using scene graphs. In *Proceedings of CVPR*, pages 3668–3678, 2015. 1
- [11] Karin Kipper, Anna Korhonen, Neville Ryant, and Martha Palmer. Extending verbnet with novel verb classes. In *LREC*, pages 1027–1032, 2006. 3
- [12] Ranjay Krishna, Yuke Zhu, Oliver Groth, Justin Johnson, Kenji Hata, Joshua Kravitz, Stephanie Chen, Yannis Kalantidis, Li-Jia Li, David A Shamma, et al. Visual genome: Connecting language and vision using crowdsourced dense image annotations. *IJCV*, 123(1):32–73, 2017. 2, 12
- [13] Rongjie Li, Songyang Zhang, Bo Wan, and Xuming He. Bipartite graph network with adaptive message passing for unbiased scene graph generation. In *Proceedings of CVPR*, pages 11109–11119, 2021. 2, 6, 7
- [14] Yikang Li, Wanli Ouyang, Bolei Zhou, Kun Wang, and Xiaogang Wang. Scene graph generation from objects, phrases and region captions. In *Proceedings of ICCV*, pages 1261–1270, 2017.
- [15] Tsung-Yi Lin, Piotr Dollár, Ross Girshick, Kaiming He, Bharath Hariharan, and Serge Belongie. Feature pyramid networks for object detection. In *Proceedings of CVPR*, pages 2117–2125, 2017. 6
- [16] Tsung-Yi Lin, Priya Goyal, Ross Girshick, Kaiming He, and Piotr Dollár. Focal loss for dense object detection. In *Pro*ceedings of ICCV, pages 2980–2988, 2017. 7
- [17] Xin Lin, Changxing Ding, Jinquan Zeng, and Dacheng Tao. Gps-net: Graph property sensing network for scene graph generation. In *Proceedings of CVPR*, pages 3746–3753, 2020. 2, 6, 7
- [18] Cewu Lu, Ranjay Krishna, Michael Bernstein, and Li Fei-Fei. Visual relationship detection with language priors. In Proceedings of ECCV, pages 852–869. Springer, 2016. 2
- [19] George A Miller. Wordnet: a lexical database for english. *Communications of the ACM*, 38(11):39–41, 1995. 3
- [20] Shaoqing Ren, Kaiming He, Ross Girshick, and Jian Sun. Faster r-cnn: Towards real-time object detection with region proposal networks. *Proceedings of NIPS*, 28:91–99, 2015. 6

- [21] Mohammed Suhail, Abhay Mittal, Behjat Siddiquie, Chris Broaddus, Jayan Eledath, Gerard Medioni, and Leonid Sigal. Energy-based learning for scene graph generation. In Proceedings of the IEEE/CVF Conference on Computer Vision and Pattern Recognition, pages 13936–13945, 2021. 6
- [22] Kaihua Tang, Yulei Niu, Jianqiang Huang, Jiaxin Shi, and Hanwang Zhang. Unbiased scene graph generation from biased training. In *Proceedings of CVPR*, pages 3716–3725, 2020. 2, 5, 6, 7
- [23] Kaihua Tang, Hanwang Zhang, Baoyuan Wu, Wenhan Luo, and Wei Liu. Learning to compose dynamic tree structures for visual contexts. In *Proceedings of CVPR*, pages 6619– 6628, 2019. 2, 5, 6, 7
- [24] Damien Teney, Lingqiao Liu, and Anton van Den Hengel. Graph-structured representations for visual question answering. In *Proceedings of CVPR*, pages 1–9, 2017.
- [25] Alvin Wan, Lisa Dunlap, Daniel Ho, Jihan Yin, Scott Lee, Henry Jin, Suzanne Petryk, Sarah Adel Bargal, and Joseph E Gonzalez. Nbdt: Neural-backed decision trees. arXiv preprint arXiv:2004.00221, 2020. 3
- [26] Sijin Wang, Ruiping Wang, Ziwei Yao, Shiguang Shan, and Xilin Chen. Cross-modal scene graph matching for relationship-aware image-text retrieval. In *Proceedings of WACV*, pages 1508–1517, 2020.
- [27] Saining Xie, Ross Girshick, Piotr Dollár, Zhuowen Tu, and Kaiming He. Aggregated residual transformations for deep neural networks. In *Proceedings of CVPR*, pages 1492–1500, 2017. 6
- [28] Danfei Xu, Yuke Zhu, Christopher B Choy, and Li Fei-Fei. Scene graph generation by iterative message passing. In *Proceedings of CVPR*, pages 5410–5419, 2017. 2, 5, 12
- [29] Shaotian Yan, Chen Shen, Zhongming Jin, Jianqiang Huang, Rongxin Jiang, Yaowu Chen, and Xian-Sheng Hua. Pcpl: Predicate-correlation perception learning for unbiased scene graph generation. In *Proceedings of ACM Multimedia*, pages 265–273, 2020. 2, 6
- [30] Xu Yang, Kaihua Tang, Hanwang Zhang, and Jianfei Cai. Auto-encoding scene graphs for image captioning. In *Proceedings of CVPR*, pages 10685–10694, 2019.
- [31] Yuan Yao, Ao Zhang, Xu Han, Mengdi Li, Cornelius Weber, Zhiyuan Liu, Stefan Wermter, and Maosong Sun. Visual distant supervision for scene graph generation. *arXiv preprint arXiv:2103.15365*, 2021. 3
- [32] Jing Yu, Yuan Chai, Yujing Wang, Yue Hu, and Qi Wu. Cogtree: Cognition tree loss for unbiased scene graph generation. arXiv preprint arXiv:2009.07526, 2020. 2, 4, 5, 6
- [33] Alireza Zareian, Svebor Karaman, and Shih-Fu Chang. Bridging knowledge graphs to generate scene graphs. In European Conference on Computer Vision, pages 606–623. Springer, 2020. 6
- [34] Rowan Zellers, Mark Yatskar, Sam Thomson, and Yejin Choi. Neural motifs: Scene graph parsing with global context. In *Proceedings of CVPR*, pages 5831–5840, 2018. 1, 2, 3, 4, 5, 6, 7
- [35] Ji Zhang, Yannis Kalantidis, Marcus Rohrbach, Manohar Paluri, Ahmed Elgammal, and Mohamed Elhoseiny. Largescale visual relationship understanding. In *Proceedings of the AAAI*, volume 33, pages 9185–9194, 2019. 3, 7, 12

[36] Bohan Zhuang, Qi Wu, Chunhua Shen, Ian Reid, and Anton van den Hengel. Hcvrd: a benchmark for large-scale human-centered visual relationship detection. In *Proceedings of AAAI*, 2018. 3

A. VG-1800 Dataset

The VG-1800 dataset aims to provide reliable evaluation for the large-scale scene graph generation.

A.1. Dataset Construction

We construct the dataset based on original Visual Genome dataset [12] by the following steps: (1) **Filtration.** Instead of simply auto-filtering [35] and choosing the top frequent predicate categories [1], we manually filter out unreasonable predicate categories, including misspelling predicates (e.g., i frot of), adjectives (e.g., white), nouns (e.g., car), and relative clauses (e.g., who has). To provide enough relation instances for robust evaluation, we retain all object categories and predicate categories with over 5 samples. (2) **Split.** We split the VG dataset into 70% training and 30% test. Following VG-50 split [28], we further split out 5,000 images from the training set as the validation set, and ensure at least 5 samples on the test set and at least 1 samples on the training set for each predicate category.

A.2. Dataset Statistics

Finally, the dataset contains 70,098 object categories, 1,807 predicate categories and 272,084 distinct relation triplets. It consists of 66,289, 4,995, and 32,893 images for training set, validation set and test set respectively. There are on average 19.5 objects and 16.0 relations for each image.

We also com-Comparison with Other VG Splits. pare our VG-1800 split with other splits based on Visual Genome [12] dataset, including a conventional VG-50 and the other two large-scale SGG splits VG8K and VG8K-LT. Our VG-1800 can provide a more reliable evaluation for large-scale SGG. (1) When compared with VG8K, we provide a much cleaner dataset by manually cleaning the noise. For example, VG8K does not filter out nouns and adjectives, which will lead to an unreliable evaluation. (2) When compared with VG8K-LT, a cleaner version of VG8K, we provide a much stable evaluation for large amount of tail classes. More specifically, as shown in Table 3, our VG-1800 contains more test images. Meanwhile, VG-1800 also contains more samples of tail classes. As shown in Figure 10, our VG-1800 has 1,807 predicate classes with no less than 5 samples, while VG8K-LT has only 526 classes that have no less than 5 samples.

B. Supplementary Experiments

Influence of k_I . To provide a more detailed analysis on the influence of k_I , we report the performance on Acc and mAcc with different k_I . As shown in Figure 9, with the increase of internal transfer percentage k_I , Acc decreases

Dataset	Filtration	Train	Val	Test	
VG-50 [28]	-	57,723	5,000	26,446	
VG8K [35]	Auto	97,961	2,000	4,871	
VG8K-LT [1]	Auto	97,623	1,999	4,860	
VG-1800	Manual	66,289	4,995	32,893	

Table 3. Comparison between different datasets' predicate filtration and split ratio. Filtration denotes the method to remove noisy predicates. The Train, Val, and Test denote number of images in training set, validation set and test set.

linearly, while mAcc first increases when $k_I \le 80\%$ and then decreases. The phenomenon shows that transferring more in internal transfer does not necessarily mean higher mAcc. For VG-1800, The first 80% internal data transfer is helpful to improve mAcc, while the last confident 20% will harm the overall performance. We guess the last 20% data may contain too noise, which will lower the data quality for model training.

Influence of k_E . As for k_E , external transfer shows almost no influence on Acc and mAcc when $k_E \leq 90\%$, while significantly boost mAcc when $k_E = 100\%$. Contrary to our observations for k_I , the last 10% samples which are believed to be unuseful by models, seem to bring the most profitable boost for mAcc. We guess the reason is that model can not distinguish well between tail classes and NA samples, while this part of the data is essential to provide more training samples for tail classes.

Adaptive Threshold. In our IETrans, when determining how much data to transfer, we equally use a fixed percentage number for all relational triplets, which seems to be suboptimal. Thus, we also tried an adaptive threshold by considering the prediction score of concrete relational triplet instances.

For internal transfer, given a general relational triplet instance (o_s, p_G, o_o) , we are required to decide whether to transfer to its corresponding informative type p_I . We denote the model's prediction score of object pair (o_s, o_o) on p_I as $s_{p_I}^*$. We denote the average and standard error of all (c_{o_s}, p_I, c_{o_o}) relational triplet instances' prediction score on p_I as μ_I and σ_I . We conduct the transfer when $s_{p_I}^*$ satisfies:

$$s_{p_I}^* > \mu_I + k\sigma_I, \tag{8}$$

where k is a hyperparameter. The intuition is that if a general instance (o_s, p_G, o_o) 's prediction score is over the average of all real (c_{o_s}, p_I, c_{o_o}) 's prediction scores on p_I , (o_s, p_G, o_o) can probably be relabeled as an informative one. Meanwhile, the standard error is considered to further control the adaptive threshold.

By choosing different k including $\{-1.0, -0.5, 0.0, 0.5, 1.0\}$, we can get a curve with different Acc and mAcc trade-offs. As shown in Figure 11,

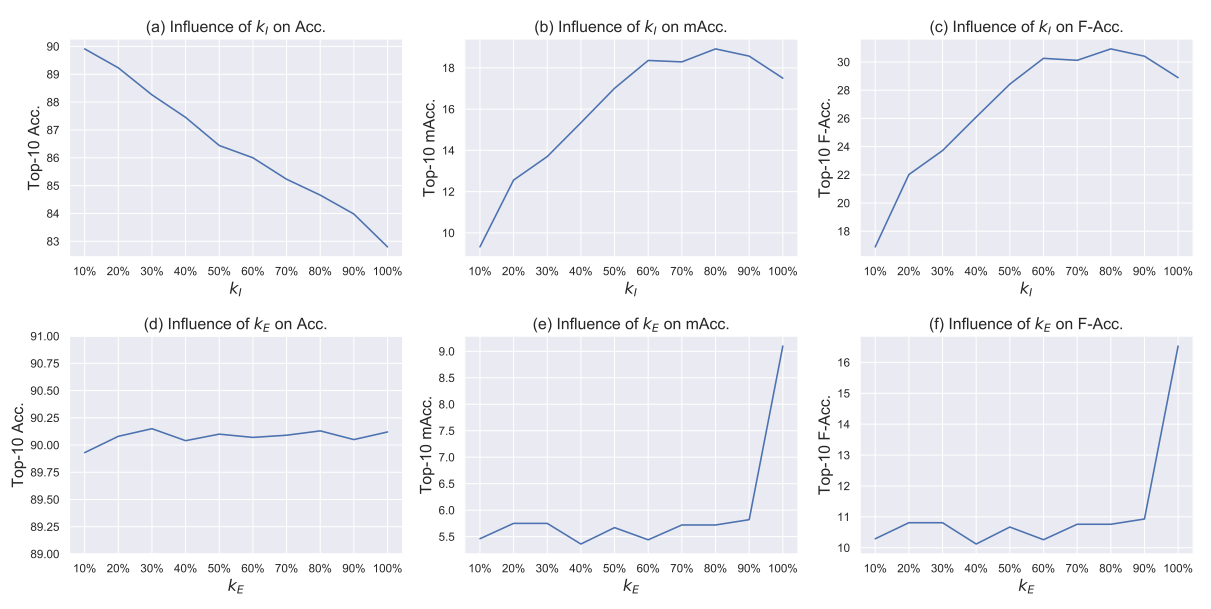


Figure 9. Influence of k_I and k_E in different metrics.

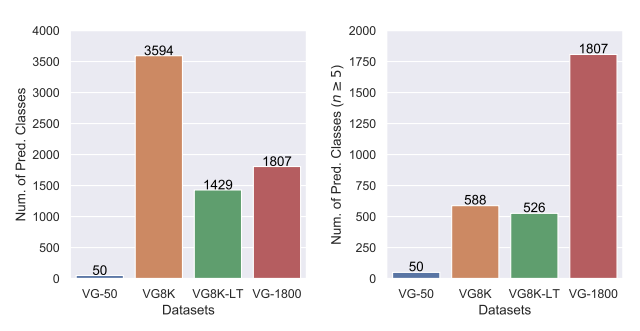


Figure 10. Comparison of number of predicate classes between different splits on test set. The $n\geq 5$ denotes predicate classes having no less than 5 samples.

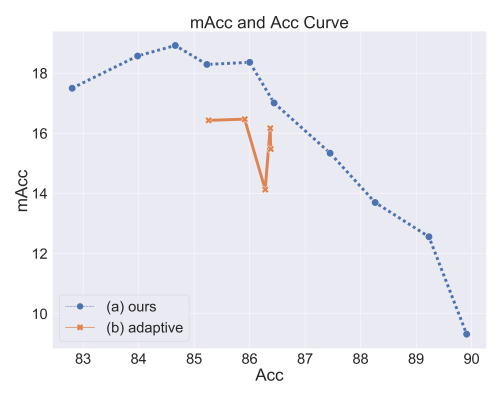


Figure 11. Comparison of adaptive thresholds and fixed percentages for Internal Transfer.

the model with adaptive thresholds is overall worse than our fixed percentage.

A possible explanation is that the prediction score of an

instance is non-linearly dependent on the number of its own instances and its similarity with different general classes, which results in inconsistency among different relational triplets. Especially when the number of an informative relational triplet is very small, the average of its prediction score is often near to zero, which will easily lead to an overtransfer problem. Thus, we leave the design of a more intelligent adaptive threshold for future work.

For external transfer, as shown in the paper, the prediction scores on NA of missed annotated samples are unreliable, i.e. the samples with the highest NA score bring maximum benefits for the model's performance.

C. Discovered Visual Hierarchy Visualization

In this section, we show 100 discovered general-informative pairs for both VG-50 and VG-1800. The pairs are ranked by the number of samples which are transferred.

Table 4: Examples of discovered visual hierarchy in VG-50

$(window, on, building) \rightarrow (window, part of, building)$	$(man, wearing, arm) \rightarrow (man, wears, arm)$
$(boy, wearing, boy) \rightarrow (boy, wears, boy)$	$(pillow, on, bed) \rightarrow (pillow, lying on, bed)$
$(building, has, building) \rightarrow (building, made of, building)$	$(sign, on, building) \rightarrow (sign, mounted on, building)$
$(arm, of, arm) \rightarrow (arm, belonging to, arm)$	$(sign, on, building) \rightarrow (sign, hanging from, building)$
$(man, wearing, bag) \rightarrow (man, wears, bag)$	$(window, on, building) \rightarrow (window, belonging to, building)$
$(car, on, building) \rightarrow (car, parked on, building)$	$(clock, on, building) \rightarrow (clock, mounted on, building)$
$(man, wearing, building) \rightarrow (man, wears, building)$	$(man, has, arm) \rightarrow (man, wears, arm)$
$(man, wearing, boot) \rightarrow (man, wears, boot)$	$(bottle, on, bottle) \rightarrow (bottle, sitting on, bottle)$
$(window, on, bus) \rightarrow (window, belonging to, bus)$	$(book, on, book) \rightarrow (book, above, book)$
$(man, has, arm) \rightarrow (man, with, arm)$	$(ear, of, ear) \rightarrow (ear, belonging to, ear)$
$(hand, of, arm) \rightarrow (hand, belonging to, arm)$	$(bottle, on, bottle) \rightarrow (bottle, above, bottle)$
$(window, in, building) \rightarrow (window, part of, building)$	$(light, on, building) \rightarrow (light, mounted on, building)$
$(door, on, building) \rightarrow (door, to, building)$	$(food, on, food) \rightarrow (food, lying on, food)$
$(bowl, on, bowl) \rightarrow (bowl, above, bowl)$	$(man, wearing, man) \rightarrow (man, wears, man)$
$(flower, in, flower) \rightarrow (flower, painted on, flower)$	$(woman, wearing, bag) \rightarrow (woman, wears, bag)$
$(tree, near, building) \rightarrow (tree, in front of, building)$	$(woman, wearing, arm) \rightarrow (woman, wears, arm)$
$(window, of, building) \rightarrow (window, part of, building)$	$(clock, on, building) \rightarrow (clock, part of, building)$
$(bus, on, building) \rightarrow (bus, parked on, building)$	$(man, wearing, coat) \rightarrow (man, wears, coat)$
$(building, has, building) \rightarrow (building, with, building)$	$(boy, wearing, arm) \rightarrow (boy, wears, arm)$
$(man, on, arm) \rightarrow (man, riding, arm)$	$(tree, has, branch) \rightarrow (tree, with, branch)$
$(woman, wearing, boot) \rightarrow (woman, wears, boot)$	$(pillow, on, bed) \rightarrow (pillow, above, bed)$
$(woman, has, arm) \rightarrow (woman, with, arm)$	$(window, on, building) \rightarrow (window, to, building)$
$(glass, on, bottle) \rightarrow (glass, sitting on, bottle)$	$(sign, on, building) \rightarrow (sign, says, building)$
$(man, wearing, bike) \rightarrow (man, wears, bike)$	$(tire, on, building) \rightarrow (tire, on back of, building)$
$(branch, on, branch) \rightarrow (branch, growing on, branch)$	$(book, on, book) \rightarrow (book, laying on, book)$
$(car, on, car) \rightarrow (car, parked on, car)$	$(man, wearing, bench) \rightarrow (man, wears, bench)$
$(elephant, has, ear) \rightarrow (elephant, using, ear)$	$(person, on, beach) \rightarrow (person, standing on, beach)$
$(wing, on, plane) \rightarrow (wing, attached to, plane)$	$(windshield, on, building) \rightarrow (windshield, of, building)$
$(arm, on, arm) \rightarrow (arm, belonging to, arm)$	$(woman, holding, bag) \rightarrow (woman, carrying, bag)$
$(window, on, bike) \rightarrow (window, part of, bike)$	$(ear, on, ear) \rightarrow (ear, belonging to, ear)$
$(man, on, beach) \rightarrow (man, walking on, beach)$	$(boy, has, boy) \rightarrow (boy, wears, boy)$
$(roof, on, building) \rightarrow (roof, covering, building)$	$(leaf, on, branch) \rightarrow (leaf, growing on, branch)$
$(head, of, arm) \rightarrow (head, belonging to, arm)$	$(wheel, on, building) \rightarrow (wheel, on back of, building)$
$(tree, near, building) \rightarrow (tree, along, building)$	$(bird, on, bird) \rightarrow (bird, sitting on, bird)$
$(door, on, door) \rightarrow (door, to, door)$	$(woman, has, bag) \rightarrow (woman, with, bag)$
$(man, wearing, hat) \rightarrow (man, wears, hat)$	$(man, on, arm) \rightarrow (man, standing on, arm)$
$(sign, on, building) \rightarrow (sign, attached to, building)$	$(letter, on, building) \rightarrow (letter, painted on, building)$
$(bird, on, bird) \rightarrow (bird, standing on, bird)$	$(ear, of, cat) \rightarrow (ear, belonging to, cat)$
$(window, on, bench) \rightarrow (window, part of, bench)$	$(window, near, building) \rightarrow (window, part of, building)$
$(wheel, on, bike) \rightarrow (wheel, on back of, bike)$	$(building, near, building) \rightarrow (building, across, building)$
$(elephant, has, ear) \rightarrow (elephant, between, ear)$	$(man, has, bag) \rightarrow (man, with, bag)$
$(engine, on, plane) \rightarrow (engine, mounted on, plane)$	$(man, wearing, chair) \rightarrow (man, wears, chair)$
$(woman, wearing, building) \rightarrow (woman, wears, building)$	$(sign, on, sign) \rightarrow (sign, mounted on, sign)$
$(plate, on, bowl) \rightarrow (plate, above, bowl)$	$(man, wearing, face) \rightarrow (man, wears, face)$
$(leg, of, giraffe) \rightarrow (leg, part of, giraffe)$	$(pillow, above, bed) \rightarrow (pillow, lying on, bed)$
$(tire, on, bike) \rightarrow (tire, on back of, bike)$	$(leg, of, arm) \rightarrow (leg, belonging to, arm)$
$(man, wearing, cap) \rightarrow (man, wears, cap)$	$(bird, has, bird) \rightarrow (bird, with, bird)$
$(trunk, of, ear) \rightarrow (trunk, belonging to, ear)$	$(roof, of, building) \rightarrow (roof, covering, building)$
$(plate, on, bottle) \rightarrow (plate, above, bottle)$	$(man, wearing, ear) \rightarrow (man, wears, ear)$
$(man, has, building) \rightarrow (man, wears, building)$	$(window, on, arm) \rightarrow (window, part of, arm)$

Table 5: Examples of discovered visual hierarchy in VG-1800

$(window, on, building) \rightarrow (window, on exterior of, building)$	$(man, wearing, arm) \rightarrow (man, wearing striped, arm)$
$(arm, of, arm) \rightarrow (arm, stretched out on, arm)$	$(man, has, arm) \rightarrow (man, stretching out, arm)$
$\frac{(alm, oi, alm)}{(cloud, in, cloud)} \rightarrow \frac{(cloud, floating through, cloud)}{(cloud, in, cloud)}$	(pillow, on, bed) \rightarrow (pillow, propped up on, bed)
$(tree, in, background) \rightarrow (tree, visible in, background)$	$(leg, of, arm) \rightarrow (leg, belonging to, arm)$
$\frac{(boat, in, boat) \rightarrow (boat, sailing on, boat)}{(boat, in, boat) \rightarrow (boat, sailing on, boat)}$	$(building, has, building) \rightarrow (building, seen outside, building)$
$(cloud, in, building) \rightarrow (cloud, floating through, building)$	(hand, of, arm) \rightarrow (hand, hand of, arm)
(boat, on, boat) \rightarrow (boat, sailing on, boat)	$(cloud, in, sky) \rightarrow (cloud, floating through, sky)$
$(boul, on, boul) \rightarrow (boul, salling on, boul)$ $(building, in, background) \rightarrow (building, visible in, background)$	$(man, has, arm) \rightarrow (man, sheltering, arm)$
$\frac{(man, wearing, arm) \rightarrow (man, dressed in, arm)}{(man, base arm)} \rightarrow (man, dressed in, arm)$	$(head, of, arm) \rightarrow (head, turning, arm)$
$(man, has, arm) \rightarrow (man, losing, arm)$	$(cloud, in, airplane) \rightarrow (cloud, floating through, airplane)$
$(cloud, in, background) \rightarrow (cloud, floating through, background)$	$(window, on, awning) \rightarrow (window, on exterior of, awning)$
$(man, has, arm) \rightarrow (man, pointing with, arm)$	$(man, has, arm) \rightarrow (man, spreading, arm)$
$(window, on, bus) \rightarrow (window, lining side of, bus)$	$(window, on, balcony) \rightarrow (window, on exterior of, balcony)$
$(cloud, in, beach) \rightarrow (cloud, floating through, beach)$	$(car, on, building) \rightarrow (car, driving alongside, building)$
$(window, on, building) \rightarrow (window, lining side of, building)$	$(man, wearing, arm) \rightarrow (man, lifting up, arm)$
$(shirt, on, arm) \rightarrow (shirt, worn by, arm)$	$(man, wearing, bag) \rightarrow (man, wearing striped, bag)$
(bottle, on, bottle) → $(bottle, kept on, bottle)$	(man, wearing, background) → (man, wearing striped, background)
$(boy, wearing, boy) \rightarrow (boy, striped, boy)$	$(cloud, in, air) \rightarrow (cloud, floating through, air)$
$(woman, has, arm) \rightarrow (woman, raising, arm)$	$(car, on, building) \rightarrow (car, moving down, building)$
$(airplane, in, airplane) \rightarrow (airplane, flying under, airplane)$	$(tile, on, bathroom) \rightarrow (tile, fixed to, bathroom)$
$(arm, on, arm) \rightarrow (arm, stretched out on, arm)$	$(cloud, in, arm) \rightarrow (cloud, floating through, arm)$
$(head, of, arm) \rightarrow (head, belonging to, arm)$	$(man, wearing, arm) \rightarrow (man, kicking up, arm)$
$(airplane, on, airplane) \rightarrow (airplane, taking off from, airplane)$	$(sign, on, building) \rightarrow (sign, strapped, building)$
$(man, wearing, air) \rightarrow (man, wearing striped, air)$	$(sign, on, arrow) \rightarrow (sign, strapped, arrow)$
$(window, on, building) \rightarrow (window, adorning, building)$	$(cat, has, cat) \rightarrow (cat, possesses, cat)$
$(cloud, in, boat) \rightarrow (cloud, floating through, boat)$	$(person, has, arm) \rightarrow (person, stretching out, arm)$
$(clock, on, building) \rightarrow (clock, attached to side of, building)$	$(train, on, building) \rightarrow (train, switching, building)$
$(woman, has, arm) \rightarrow (woman, combing, arm)$	(boy, wearing, arm) o (boy, striped, arm)
$(window, on, building) \rightarrow (window, on the side of, building)$	$(window, of, building) \rightarrow (window, on exterior of, building)$
$(arrow, on, arrow) \rightarrow (arrow, printed, arrow)$	$(woman, wearing, arm) \rightarrow (woman, wearing striped, arm)$
$(head, of, arm) \rightarrow (head, turned to, arm)$	$(branch, on, branch) \rightarrow (branch, sticking up on, branch)$
$(man, on, arm) \rightarrow (man, swimming with, arm)$	$(wing, on, airplane) \rightarrow (wing, on left side of, airplane)$
$(mountain, in, background) \rightarrow (mountain, visible in, background)$	$(bowl, on, bowl) \rightarrow (bowl, placed on, bowl)$
$(cloud, in, blue sky) \rightarrow (cloud, floating through, blue sky)$	$(window, on, arrow) \rightarrow (window, on exterior of, arrow)$
$(foot, of, arm) \rightarrow (foot, belonging to, arm)$	$(toilet, in, bathroom) \rightarrow (toilet, installed in, bathroom)$
$(sign, on, building) \rightarrow (sign, anchored to, building)$	$(wall, on, building) \rightarrow (wall, making up, building)$
$(kite, in, air) \rightarrow (kite, flying through, air)$	$(leaf, on, building) \rightarrow (leaf, growing on, building)$
$(man, wearing, arm) \rightarrow (man, adjusting, arm)$	$(person, wearing, arm) \rightarrow (person, striped, arm)$
$(tile, on, bathroom) \rightarrow (tile, installed on, bathroom)$	$(bag, on, bag) \rightarrow (bag, kept in, bag)$
$(sky, in, sky) \rightarrow (sky, stretched across, sky)$	$(bear, has, bear) \rightarrow (bear, scratching, bear)$
$(line, on, building) \rightarrow (line, painted in, building)$	$(man, wearing, building) \rightarrow (man, wearing striped, building)$
$(book, on, book) \rightarrow (book, arranged on, book)$	$(wall, near, building) \rightarrow (wall, making up, building)$
$(window, on, advertisement) \rightarrow (window, lining side of, advertisement)$	$(sink, in, bathroom) \rightarrow (sink, mounted in, bathroom)$
$(wave, in, arm) \rightarrow (wave, cresting in, arm)$	(window, in, building) \rightarrow (window, on exterior of, building)
$\frac{(blanket, on, bed) \rightarrow (blanket, laying over, bed)}{(blanket, on, bed)}$	$(man, wearing, backpack) \rightarrow (man, carrying, backpack)$
$\frac{(hair, of, arm) \rightarrow (hair, on head of, arm)}{(hair, of, arm)}$	$(kite, in, beach) \rightarrow (kite, kite in, beach)$
$(man, wearing, arm) \rightarrow (man, dressed, arm)$	$(boy, has, arm) \rightarrow (boy, outstretched, arm)$
$(picture, on, bed) \rightarrow (picture, framed on, bed)$	$(window, on, banner) \rightarrow (window, on exterior of, banner)$
$(arm, of, arm) \rightarrow (arm, belonging to, arm)$	$(man, on, board) \rightarrow (man, going off, board)$
$(shadow, on, arm) \rightarrow (shadow, cast over, arm)$	$(arm, of, arm) \rightarrow (arm, around neck of, arm)$
(Simulon, Cit, with) / (Simulon, Case Over, with)	(wint, or, wint) / (wint, around neon or, wint)